The Swing Adsorption Reactor Cluster (SARC) for Post Combustion CO_2 Capture: Experimental Proof-of-Principle

Chaitanya Dhoke[1], Abdelghafour Zaabout[2], Schalk Cloete[2], Hwimin Seo[3], Yong-ki Park[3], Richard Blom[4], Shahriar Amini[1,2]*

[1] *Norwegian University of Science and Technology, Trondheim, Norway;*

[2] *SINTEF industry, Trondheim, Norway;*

[3] *Korean Research Institute for Chemical Technology, Daejeon, South Korea;*

[4] *SINTEF industry, Oslo, Norway*

*Corresponding author:

Name: A*bdelghafour Zaabout*

S.P. Andersensvei 15b, 7031, Trondheim, Norway

Phone: +47 93008204

Email : *abdelghafour.zaabout@sintef.no*

Abstract

This paper presents the first experimental demonstration of the novel swing adsorption reactor cluster (SARC) for post combustion CO_2 capture. The SARC concept combines a temperature and vacuum swing for sorbent regeneration. A heat pump is used for transferring heat from the exothermic carbonation reaction to the endothermic regeneration reaction. Sorbent regeneration under vacuum allows for a small temperature difference between carbonation and regeneration, leading to a high heat pump efficiency. This key principle behind the SARC concept was demonstrated through lab-scale experiments comparing combined vacuum and temperature swing adsorption (VTSA) to pure temperature swing adsorption (TSA), showing that a 50 mbar vacuum can reduce the required temperature swing by 30-40 °C. A complete SARC cycle comprising of carbonation, evacuation, regeneration and cooling steps was also demonstrated. The cycle performed largely as expected, although care had to be taken to avoid particle elutriation under vacuum and the CO_2 release rate was relatively slow. The SARC principle has therefore been successfully proven and further scale-up efforts are strongly recommended.

Keywords: Post combustion CO_2 capture; Adsorption; Combined vacuum and temperature swing; Fluidized bed

Abbreviation

SARC	Swing adsorption reactor cluster
VSA	Vacuum swing adsorption
VTSA	Vacuum combine temperature swing adsorption
TSA	Temperature swing adsorption
PSA	Pressure swing adsorption
CCUS	Carbon dioxide capture, utilization and storage
CaL	Calcium looping
COP	Coefficient of performance
P&ID	Process and instrumentation diagram

MFC	Mass flow controller
PEI	Polyethyleneimine
KRICT	Korean Research Institute for Chemical Technology
LPM	Liters /minutes

1 Introduction

According to the latest IPCC report [1], CO_2 capture, utilization and storage (CCUS) will play a major role in cost effective mitigation of climate change caused by anthropogenic CO_2 emissions. Tremendous research efforts have been deployed to applying CCUS for capturing CO_2 from a wide spectrum of industrial applications covering power production [2-4] and CO_2 intensive industries [4-6].

Post combustion CO_2 capture offers the opportunity for abating CO_2 emissions from CO_2 intensive sources such as steel making and cement plants, as well as from new and existing power plants, and promises a broad deployment as soon as a governmental carbon tax scheme is implemented. Amine scrubbing is the most mature of these technologies, but still imposes a high energy penalty on CO_2 capture despite implementation of all possible heat and process integration configurations (7-12 %-points on coal power plants [7-10]).

Adsorption based technologies have the potential to bring down the energy penalty of post combustion CO_2 capture [11]. Specifically, low temperature adsorption-based technologies are especially attractive because they can easily be retrofitted into existing plants with minimal interaction [12]. These processes can operate with a pressure swing VSA/PSA configuration, using mainly physisorption based sorbents (operated in a fixed bed reactor) [13, 14], or with a temperature swing TSA configuration using mainly chemisorption-based sorbents [15]. Each configuration has its own pros and cons, but the latter usually has a high CO_2 adsorption capacity and selectivity, in addition to high tolerance to water [12]. The associated CO_2 capture energy penalty could, however, be high due the high regeneration energy of the chemisorption-based sorbents [16]. Tremendous research efforts have been deployed in development of chemisorption-based sorbents with minimal regeneration enthalpy and maximal CO_2 adsorption capacity, where amine functionalized

sorbent (both impregnated and grafted), have shown promise to be the most promising in this category [12]. The focus in sorbent development research has evolved to MOF (Metal Organic Framework) which exhibits CO_2 adsorption capacities as high as 5.5 mmol. g^{-1} (at 0.15 bar, 313 K) owing to their extraordinary high surface areas and pore volume [17, 18].

Conventionally, sorbent-based TSA uses an interconnected fluidized bed configuration operating at two different temperatures where the sorbent undergoes a temperature swing, adsorbing CO_2 in the low temperature reactor to release it in the high temperature reactor [19, 20]. The main challenge with this configuration is that the co-current flow in the riser makes it difficult to meet the 90% CO_2 capture criterion and results in small working adsorption capacities, . Other reactor configurations have been proposed mainly to solve this issue by adopting multistage co- and counter-current risers in the carbonator [21-23], enabling contacting the gas stream with decreasing CO_2 partial pressure with fresher sorbent. Other reactor configurations considered reducing the energy penalty through heat integration. This includes, the moving bed [24], the inter-stage heat integration interconnected fluidized bed [16] and the Swing Adsorption Reactor cluster (SARC) [25].

The novel SARC concept consists of a cluster of stand-alone reactors, where the sorbent in each reactor is alternately exposed to carbonation and regeneration conditions via dynamic temperature and pressure swings (Figure 1.a). A typical cycle taking place in one SARC reactor is illustrated Figure 2, showing a temperature swing of 8 °C in the reactor and a pressure swing of 0.9 bar between the carbonation and regeneration steps, as simulated using a 0D model for a SARC reactor using PEI sorbents [25]. Short evacuation and cooling steps are applied between the main carbonation and regeneration steps to maximize CO_2 purity and capture efficiency.

The temperature swing is completed using a heat pump transferring heat from carbonation to regeneration (Figure 1 .b)). As shown in Figure 2, application of a 0.1 bar vacuum can allow sorbent regeneration at very low temperature swing, implying a high heat pump efficiency ($COP \approx 0.65\, T_{cold}/(T_{hot} - T_{cold}) = 12$ in the example Figure 1 b). This temperature and vacuum swings

combination avoids the need for a two-steps VSA process needed to achieve high capture efficiency, as extreme vacuum are energetically expensive and difficult to achieve in industrial scale [26]. Efficient heat transfer via the heat pump requires a fluidized bed reactor, but axial mixing in the reactor must also be restricted to achieve high CO_2 capture rates in the carbonator. The presence of heat transfer tubes will already restrict axial mixing, although great plug flow behavior can be achieved by strategically placed baffles or a multistage reactor configuration. Note that a VTSA system has previously been tested experimentally under fixed bed conditions, which caused unrealistically long cycle time due to the poor heat transfer in fixed bed [27]. No heat integration between carbonation and regeneration was mentioned.

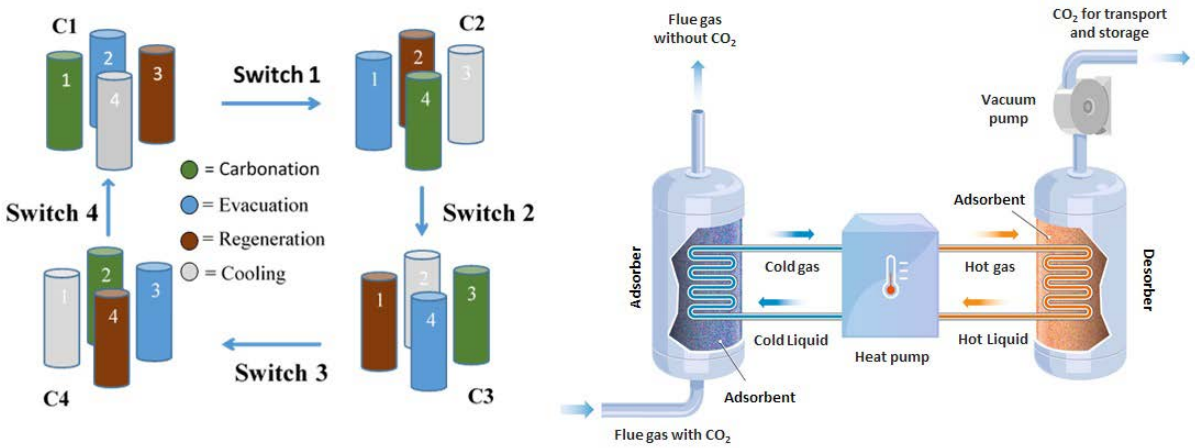

Figure 1: A conceptual design of SARC: a) a SARC cluster composed of four reactors for steady operation; b) a heat pump transferring heat between two SARC reactors in the cluster: one under carbonation and the other under regeneration

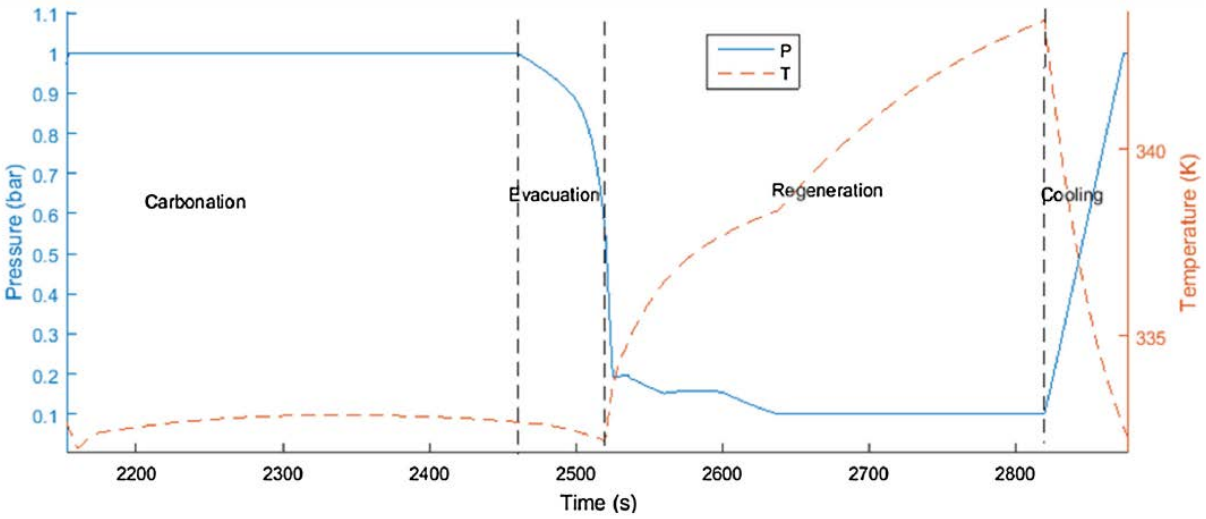

Figure 2: A typical SARC reactor cycle as simulated using a 0D model developed in [26]

Power plant simulations of the SARC concept integrated into a large scale coal-fired power plant (771 MW), have shown that energy penalties on CO_2 capture below 8 %-points could be achieved with SARC technology [25, 28] (these recent studies show a layout with detailed process requirements of SARC integration into the power plant). The footprint was however ~2x larger than that of an MEA system, but the SARC reactors will be shorter than a typical MEA absorption column, potentially resulting in competitive reactor capital costs [25, 28]. When compared to pure pressure swing adsorption, the SARC footprint was found 8x smaller, while the energy penalty is also significantly lower than the 10.3%-points [26]. Another advantage of SARC is the use of vacuum levels that are feasible at industrial scale (0.1 bar is the lowest targeted vacuum by SARC), thereby avoiding the need for the two-stages process adopted in PSA systems [26].

This paper presents an experimental proof of the SARC principle using a small-scale laboratory reactor designed and constructed for this purpose (60 g of sorbent). The experimental setups for measuring adsorption isotherms and for demonstrating SARC concept will be described first, followed by a description of the experimental campaign carried out in this study. Subsequently, results will be presented and discussed, followed by the main conclusions.

2 Methodology

2.1 Experimental setup

A lab scale reactor was constructed to carry out gas-solids reactive experiments under low temperature and vacuum conditions relevant to the SARC concept operation conditions. The reactor body has a cylindrical section of 2 cm diameter and 100 cm length with a porous plate placed at the bottom to hold the particles and uniformly distribute the gas to the reactor. The reactor was placed in a jacketed shell, wherein cooling water can be circulated, or electrical heating can be supplied. An overview of the different parts forming the setup is shown in the P&ID (Figure 3).

The reactor was heated up to the operating temperature using an external electrical heater surrounding the bottom half part of the reactor body (Figure 3) and was monitored using a thermocouple inserted into the bed from the top of the reactor. Vacuum was established inside the reactor using a vacuum pump, while the pressure was controlled using a mass flow controller (MFC3) that was placed on the reactor outlet just before the vacuum pump. A pressure sensor measuring the pressure inside the reactor was then controlling MFC3 to establish the target pressure. Gas feeds into the reactor were controlled using two mass flow controllers; MFC1 and MFC2. The experimental setup is equipped with an online syngas analyzer (ETG MCA 100 Syn Biogas Multigas Analyzer) sampling gases at the outlet of the atmospheric and vacuum vents to measure the gas composition at 1 Hz frequency.

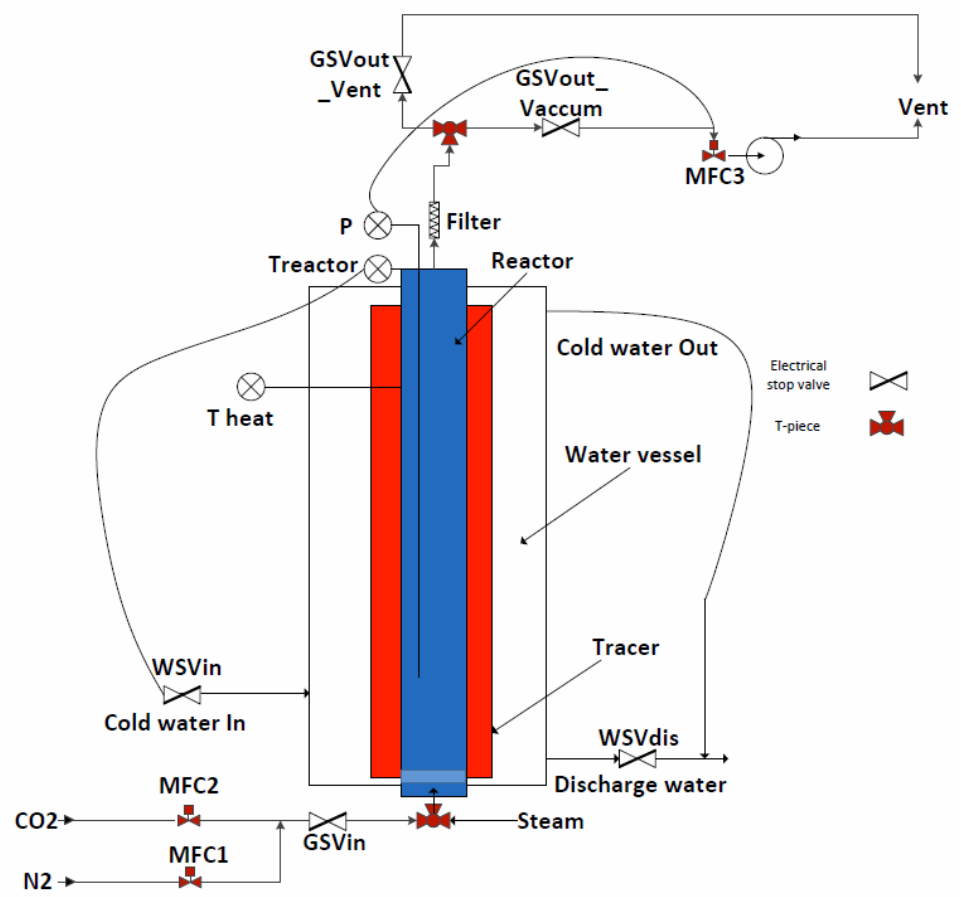

Figure 3: Experimental set up

2.2 Sorbent material

A Polyethyleneimine based (PEI) sorbent was used in this study. In general, PEI based sorbents have low regeneration enthalpies and high adsorption capacity, in addition to high selectivity to CO_2 [29].This sorbent was developed at the Korean Research Institute of Chemical Technology (KRICT) and extensively tested in a pilot scale circulating reactor configuration at KRICT [30]. The sorbent was made following impregnation of PEI on spherical commercial silica spheres [30]. The sorbent properties are depicted in Table 1. CO_2 isotherms for this sorbent were recorded on a volumetric Belsorp Max instrument in the temperature interval of 313 to 383 K, for pressures from vacuum up to 100 kPa (CO_2).

Table 1: Physical, chemical and thermochemical properties of sorbent

Sorbent composition	BET surface area (m^2/g)	Average Pore diameter (Å)	Density Skeletal (g/ml)	Density Particle (g/ml)	Adsorption enthalpy (GJ/ton CO_2)	Average Heat capacity (40-120 ^{0}C) (J/g.K)
PEI (45 wt. %) + SiO_2 (55 wt.%)	42.09	383.1	1.53	1.36	1.47	1.5

A model was fit to the experimental measurements according to the Toth isotherm (Equation 1 to Equation 4). The model parameters providing the best fit are given in Table 2 and the quality of the resulting fit is illustrated in Figure 4.

$$q = \frac{n_s b p_{CO_2}}{\left(1 - \left(b p_{CO_2}\right)^t\right)^{\frac{1}{t}}} \qquad \text{Equation 1}$$

$$b = b_0 \exp\left(\frac{dH}{RT_0}\left(\frac{T_0}{T} - 1\right)\right) \qquad \text{Equation 2}$$

$$n_s = n_{s,0} \exp\left(X\left(1 - \frac{T}{T_0}\right)\right) \qquad \text{Equation 3}$$

$$t = t_0 + \alpha\left(1 - \frac{T_0}{T}\right) \qquad \text{Equation 4}$$

Table 2: Toth isotherm parameters for the fit in Figure 4.

b_0	69.72 kPa^{-1}
dH	118.6 kJ/mol
T_0	303 K
$n_{s,0}$	2.135
X	0
t_0	0.3648
α	2.242

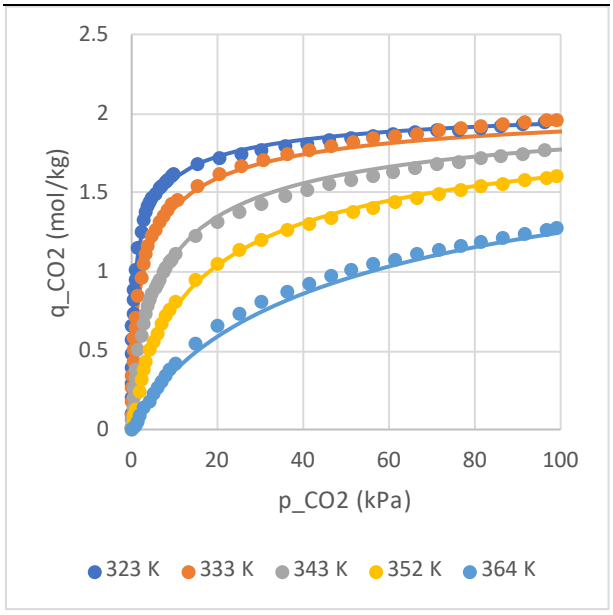

Figure 4: Illustration of the isotherm fit (Table 2) against experimental measurements at five different temperatures.

2.3 Reactor experiments

This study was structured in four experimental campaigns, summarized in Table 3, completed on 60 g of sorbent placed initially in the reactor.

The first campaign consisted of pure TSA cycles applied on fresh sorbent to investigate the possible need for sorbent activation. This study was conducted over ten successive cycles at atmospheric pressure (1000 mbar) with carbonation at 60 ^{0}C and regeneration at 120 ^{0}C. The gas composition was sampled continuously at the reactor outlet to estimate the working capacity from carbonation under conditions which is defined as in Equation 5;

$$Working\ capacity = \frac{(moles\ of\ CO_2\ desorbed - moles\ of\ CO_2\ adsorbed)\ during\ regeneration}{kg\ of\ adsorbent} \quad \text{Equation 5}$$

Table 3: Regeneration conditions over the four experimental campaigns. All experiments were completed on a bed with 60 g of sorbent, with carbonation carried out at atmospheric pressure and 60 °C using a 2 Nl/min feed of 12.5% CO_2 in N_2.

Study/ Experimental set	Objective	Mode	Regeneration Temperature range	Regeneration pressure range	Purge gas during regeneration
1	Equilibrating sorbent	TSA	120 ^{0}C	1000 mbar	N_2=0.5 LPM
2	Comparative study TSA vs. VTSA	TSA	60-120 ^{0}C	1000 mbar	CO_2=0.5 LPM
		VTSA	60-80 ^{0}C	50 mbar	NA
3	Parametric study	VTSA	60-80 ^{0}C	50-150 mbar	NA
4	SARC complete cycle	VTSA	80 ^{0}C	100 mbar	NA

The second study was designed to compare combined Vacuum –and Temperature Swing Adsorption (VTSA) to pure Temperature Swing Adsorption (TSA). The regeneration temperature was varied in 10 $^\circ$C intervals over the ranges indicated in Table 3. Gas analysis was continuously monitored in both the modes and the working capacity was quantified for comparison.

The third study investigated the effect of regeneration temperature and pressure over three levels in the ranges indicated Table 3. Each experiment was repeated three times to quantify the experimental

measurement uncertainty. The quantified working capacities from each case were compared with the isotherm model.

The last study was performed to explicitly show how the SARC process would work in practice by completing the whole SARC cycle under the VTSA mode. The sorbent was exposed to the four SARC steps in sequential manner: carbonation, evacuation, regeneration and cooling (as illustrated in Figure 8). In the carbonation step, the sorbent was exposed to 12.5 mole % of CO_2 in N_2 at 60 ^{0}C and 1000 mbar, followed by the evacuation step, wherein, 100 mbar vacuum was established at 60 ^{0}C. Subsequently, the sorbent was heated to 80 ^{0}C while maintaining the vacuum of 100 mbar for the combined vacuum-temperature swing regeneration step. Finally, the sorbent was cooled back to 60 ^{0}C while repressurizing the reactor to 1000 mbar. Gas analysis was carried out continuously and the corresponding working capacity was measured.

3 Results and Discussion

a. Sorbent working capacity and stability

The maximum working capacity over 10 cycles was measured and the results are shown in Figure 5. An average working capacity of 1.2 mol/kg of sorbent was measured for 10 consecutive cycles with a small standard deviation of 0.02 mol/kg. This result confirms the stability of the sorbent and the repeatability of the experimental procedure.

As suggested by Figure 4, the maximum sorbent working capacity is about 2 mol/kg. However, this is not achievable in practice when completing the carbonation at 60 °C and only 12.5% CO_2 because the sorbent cannot reach its maximum loading under these conditions. The 1.2 mol/kg found in this experiment is thus a good indication of the maximum sorbent working capacity under realistic operating conditions.

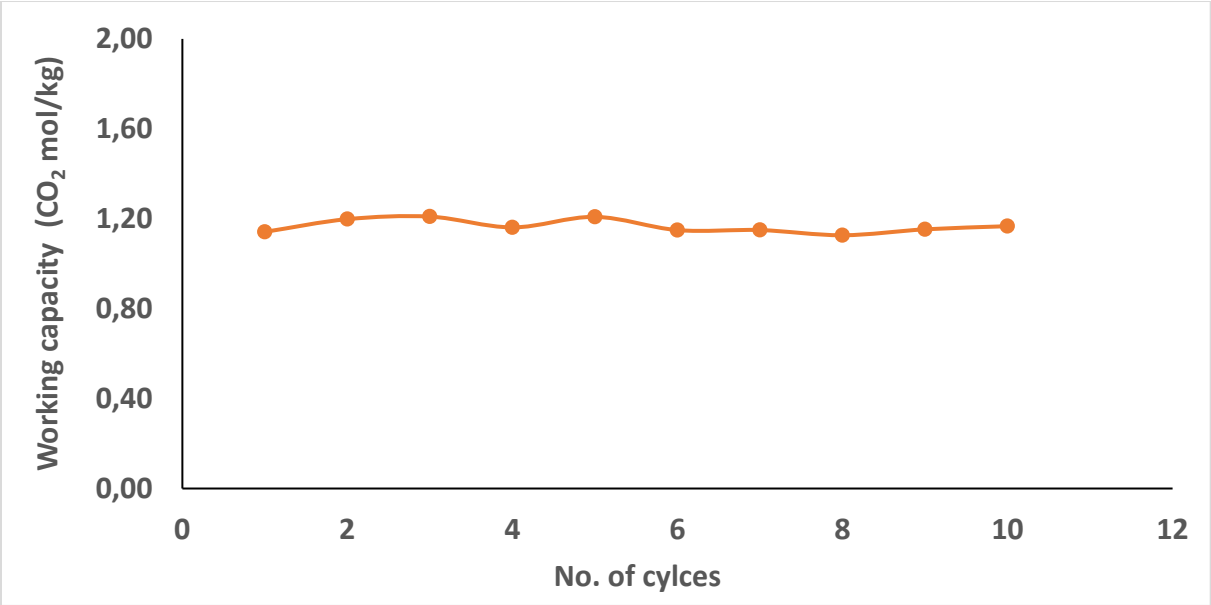

Figure 5: Sorbent working capacity over 10 consecutive cycles for the first experimental campaign in Table 3

b. Comparative study of TSA and VTSA

As seen in Figure 6, working capacity increases with increase in the regeneration temperature for both TSA and VTSA operating modes. This is expected as increase in temperature favors the desorption of CO_2. As expected, the presence of a vacuum greatly increased the achievable working capacity at a given temperature relative to pure TSA.

Another interesting result from Figure 6 is the negative working capacity for TSA at temperatures below 80 °C. In the TSA experiments, regeneration was conducted in the presence of 100% CO_2 showing that the effect of partial pressure is more dominating than the temperature (the increase in partial pressure from 12.5% to 100% of CO_2 lead to more adsorption than desorption even when the temperature was raised from 60 ^{0}C to 80 ^{0}C). At temperatures beyond 80 ^{0}C, a positive TSA working capacity indicates that temperature is dominating compared to partial pressure of CO_2.

In VTSA mode, regeneration was carried out in a vacuum of 50 mbar. In general, the results indicate that this vacuum swing can reduce the required temperature swing by 30-40 °C relative to TSA for achieving a given working capacity. This substantial reduction in temperature swing will have a large positive effect on heat pump efficiency.

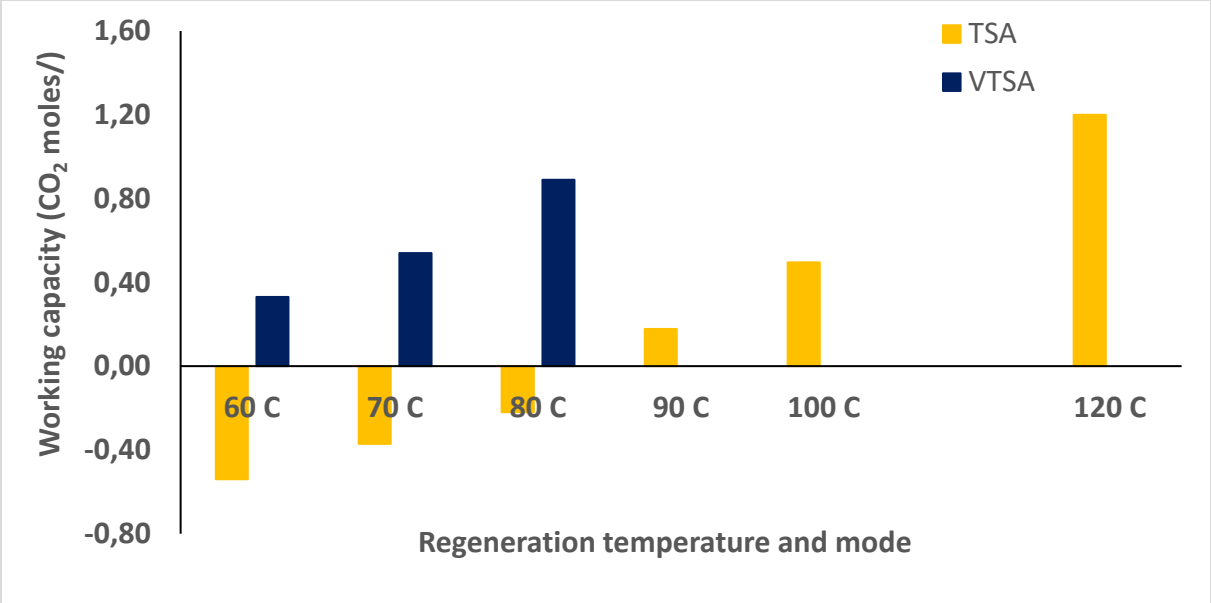

Figure 6: Comparison of TSA and VTSA following the second experimental campaign in Table 3

c. Parametric study with VTSA

As shown in Figure 7, the working capacity measured experimentally is consistent with the prediction from the isotherm model illustrated in Figure 4. Some minor deviations are observed in some cases, but this may be due to variability in the experiments as indicated by the standard deviation bars. As expected, the working capacity increases with increasing vacuum level and regeneration temperature. Within the ranges investigated in this study, the temperature has a larger effect than the vacuum.

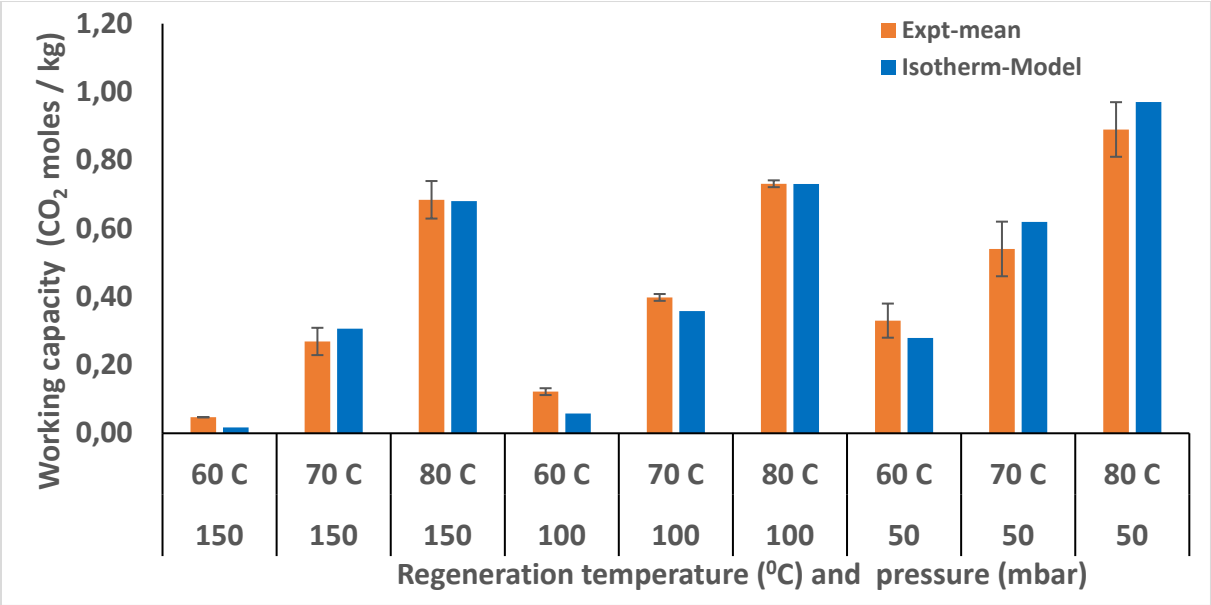

Figure 7: Parametric study on regeneration temperature and pressure following to the third experimental campaign in Table 3.

It should be noted that a pure vacuum of 50 mbar may not be practical or economical in a large-scale reactor due to sealing requirements and the size of the required vacuum pump. For sorbents that adsorb and desorb water vapor, however, a partial pressure close to 50 mbar can be achievable at a physical pressure of 100 mbar due to the release of water vapor under regeneration. However, the release of water vapor during desorption will also increase the work to be done by the vacuum pump because more gas needs to be extracted. A recent study showed that these two effects cancel out almost exactly, implying that water adsorption by the sorbent does not have a significant impact on the efficiency of the SARC process [28].

d. Complete SARC cycle

In this section, the entire SARC cycle consisting of four steps was completed by applying a temperature swing of 20 ^{0}C and a pressure swing of 900 mbar when regenerating the sorbent. As mentioned in section 2.3, evacuation and cooling steps were applied between the carbonation and regeneration steps. The carbonation time was set to capture 86.3 % of the CO_2 across the step while the regeneration time was manipulated to recover the maximum moles of CO_2 at 100 mbar and 80 ^{0}C. This was determined during the experiment by monitoring the gas analyzer signal and the regeneration step ended when the mole percentage of CO_2 approached 0 % in gas analyzer.

Figure 8 shows the process conditions for SARC cycle, where in the temperature and pressure are plotted against time for one complete SARC cycle. A slight rise in temperature (4^0C) was observed in the carbonation step due to the exothermic adsorption of CO_2 on the sorbent. Indeed, during the carbonation step, the CO_2 molar flowrate exiting the reactor is nearly zero for first 4.5 mins (Figure 9), indicating 100 % capture of CO_2. Towards the end of the carbonation step, the CO_2 slippage increases substantially as the (Figure 9).

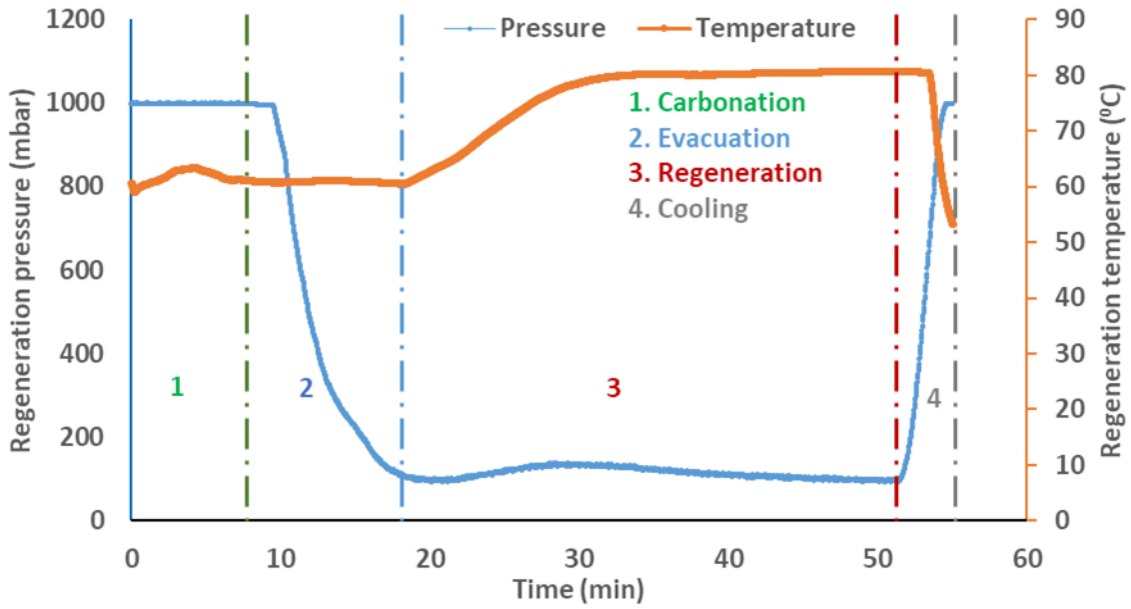

Figure 8: Pressure and temperature measurements over the SARC cycle.

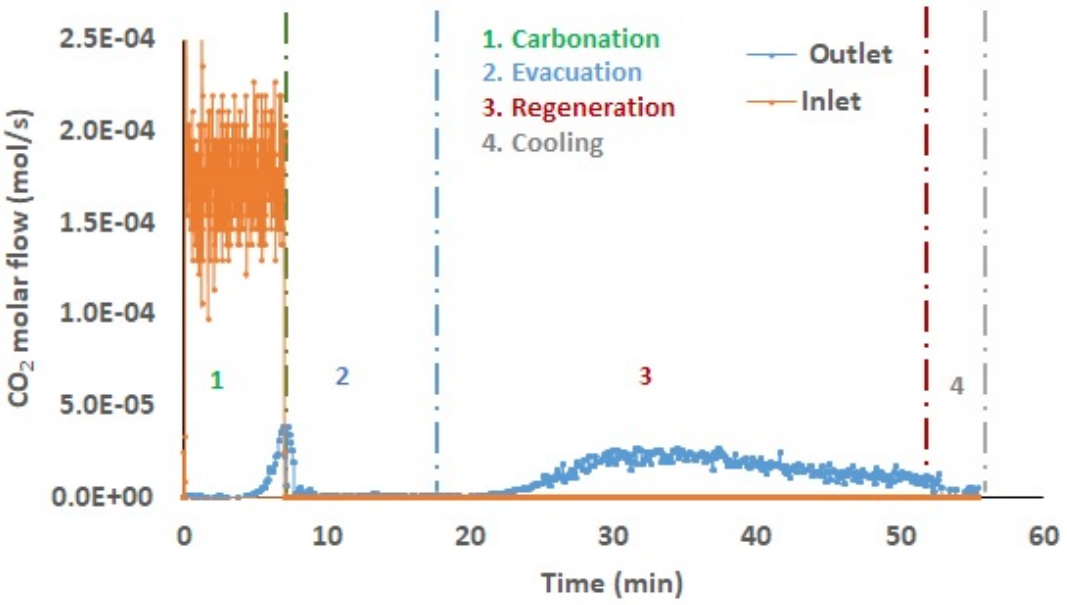

Figure 9: Molar flow of CO_2 over the SARC Cycle

In the regeneration step, the molar flow of CO_2 increased significantly when the temperature was increased from 60 to 80 °C (Figure 8 & Figure 9). A slight increase in reactor pressure was observed during regeneration due to the desorption of CO_2 as a result of the increase in temperature while maintaining the 100 mbar vacuum (Figure 8). When the target regeneration temperature was reached, the CO_2 release continued, indicating kinetic limitations in sorbent regeneration at this temperature (the sorbent required about 20 minutes to reach equilibrium). Finally, the reactor was re-pressurized to 1000 mbar and the temperature lowered to 60 °C.

It can also be pointed out that the evacuation and regeneration steps had to be carried out carefully to avoid the elutriation of particles. The vacuum conditions imposed a high flow velocity at a low mass flow rate and the flow velocity varied significantly over time. Controlling these steps to maximize the rate of regeneration, while avoiding excessive particle elutriation will be an important operating challenge for the SARC concept.

The results indicated that a working capacity of 0.55 mol/kg could be achieved with the capture of more than 85% of CO_2 when a combined VTSA (20 °C and 900 mbar) was applied compared to 1.2

mol/kg when a pure TSA of 60 °C was applied. In other words, the combination of a vacuum swing to 100 mbar and a 20 °C temperature swing could utilize almost half of the practically achievable sorbent working capacity quantified in Figure 5. This lower sorbent utilization is partly because the sorbent cannot be completely regenerated at 100 mbar and 80 °C (see Figure 6), and partly because the carbonation step had to be stopped well before the CO_2 partial pressure reached 125 mbar to avoid excessive CO_2 release. The latter effect is minimized by the large aspect ratio of the test reactor, which will restrict axial mixing, leading to more plug flow behavior during carbonation. This behavior must be replicated in larger reactor designs through baffles or a multistage reactor design.

4 Summary and conclusions

The SARC concept is a promising new post combustion CO_2 capture solution. Given that it operates only on electricity, SARC is ideally suited to retrofits into industrial applications where large quantities of steam is not available for sorbent regeneration. This concept has thus far only been investigated theoretically, and this study is the first to prove the SARC principle experimentally.

Experiments were carried out in a small lab-scale reactor over a PEI-based sorbent. The sorbent had a maximum working capacity of 2 mol/kg, but this maximum working capacity reduced to 1.2 mol/kg when considering that carbonation will take place at 60 °C with a flue gas containing only 12.5% CO_2.

The sorbent working capacity between carbonation in a stream of 12.5% CO_2 and regeneration at different levels of temperature and pressure clearly illustrated how increased vacuum swing can be traded for decreased temperature swing. In general, a vacuum swing to 50 mbar could reduce the temperature swing required for a given sorbent working capacity by 30-40 °C. This is critical to the SARC concept, which uses a heat pump for achieving the temperature swing, because a decreased temperature swing substantially increases heat pump efficiency.

A full SARC cycle of carbonation, evacuation, regeneration and cooling was demonstrated. The cycle behaved largely as expected, although care had to be taken to control the flow rate during evacuation

and regeneration to prevent particle elutriation. Regeneration also appeared relatively slow, which could result in longer regeneration times and a larger reactor footprint. A sorbent working capacity of 0.55 mol/kg was achieved over the SARC cycle, which is in line with previous modelling work of the SARC concept integrated with a coal-fired power plant [25].

The principle behind the SARC concept has therefore been successfully demonstrated experimentally and further scale-up efforts can be strongly recommended.

5 Acknowledgement

This study was performed as part of the project entitled "Demonstration of the Swing Adsorption Reactor Cluster (SARC) for simple and cost effective post-combustion CO_2 capture", funded by the Research Council of Norway under the CLIMIT program (grant no. 268507/E20). Engineers Inge Håvard Rekstad and Reidar Tellebon at VATL lab of Norwegian University of Science and Technology are acknowledged for their contribution to refining the design of the experimental set up, in addition to its construction and maintenance.

6 References

1. IPCC, *Climate change mitigation: Summary for Policymakers*. 2014.
2. Viebahn, P., D. Vallentin, and S. Holler, *Prospects of carbon capture and storage (CCS) in China's power sector - An integrated assessment.* Applied Energy, 2015. **157**: p. 229-244.
3. Rubin, E.S., et al., *The outlook for improved carbon capture technology.* Progress in Energy and Combustion Science, 2012. **38**(5): p. 630-671.
4. Cormos, A.M., et al., *Carbon capture and utilisation technologies applied to energy conversion systems and other energy-intensive industrial applications.* Fuel, 2018. **211**: p. 883-890.
5. Leeson, D., et al., *A Techno-economic analysis and systematic review of carbon capture and storage (CCS) applied to the iron and steel, cement, oil refining and pulp and paper industries, as well as other high purity sources.* International Journal of Greenhouse Gas Control, 2017. **61**: p. 71-84.
6. Bains, P., P. Psarras, and J. Wilcox, *CO2 capture from the industry sector.* Progress in Energy and Combustion Science, 2017. **63**: p. 146-172.
7. Ahn, H., et al., *Process configuration studies of the amine capture process for coal-fired power plants.* International Journal of Greenhouse Gas Control, 2013. **16**: p. 29-40.
8. Kvamsdal, H.M., et al., *Energetic evaluation of a power plant integrated with a piperazine-based CO2 capture process.* International Journal of Greenhouse Gas Control, 2014. **28**: p. 343-355.

9. Kvamsdal, H.M., et al., *Optimizing integrated reference cases in the OCTAVIUS project.* International Journal of Greenhouse Gas Control, 2016. **50**: p. 23-36.
10. Manzolini, G., et al., *Economic assessment of novel amine based CO2 capture technologies integrated in power plants based on European Benchmarking Task Force methodology.* Applied Energy, 2015. **138**: p. 546-558.
11. Zhao, M., A.I. Minett, and A.T. Harris, *A review of techno-economic models for the retrofitting of conventional pulverised-coal power plants for post-combustion capture (PCC) of CO2.* Energy & Environmental Science, 2013. **6**(1): p. 25-40.
12. Samanta, A., et al., *Post-Combustion CO2 Capture Using Solid Sorbents: A Review.* Industrial & Engineering Chemistry Research, 2012. **51**(4): p. 1438-1463.
13. Shen, C., et al., *Two-Stage VPSA Process for CO2 Capture from Flue Gas Using Activated Carbon Beads.* Industrial & Engineering Chemistry Research, 2012. **51**(13): p. 5011-5021.
14. Wang, L., et al., *CO2 capture from flue gas by two successive VPSA units using 13XAPG.* Adsorption, 2012. **18**(5): p. 445-459.
15. Lee, J.B., et al., *CO2 capture from flue gas using potassium-based dry regenerable sorbents.* Energy Procedia, 2011. **4**: p. 1494-1499.
16. Kim, K., et al., *A solid sorbent-based multi-stage fluidized bed process with inter-stage heat integration as an energy efficient carbon capture process.* International Journal of Greenhouse Gas Control, 2014. **26**: p. 135-146.
17. Bui, M., et al., *Carbon capture and storage (CCS): the way forward.* Energy & Environmental Science, 2018. **11**(5): p. 1062-1176.
18. Bae, T.H., et al., *Evaluation of cation-exchanged zeolite adsorbents for post-combustion carbon dioxide capture.* Energy & Environmental Science, 2013. **6**(1): p. 128-138.
19. Yi, C.-K., et al., *Continuous operation of the potassium-based dry sorbent CO2 capture process with two fluidized-bed reactors.* International Journal of Greenhouse Gas Control, 2007. **1**(1): p. 31-36.
20. Veneman, R., et al., *Continuous CO2 capture in a circulating fluidized bed using supported amine sorbents.* Chemical Engineering Journal, 2012. **207–208**: p. 18-26.
21. Proell, T., et al., *Introduction and evaluation of a double loop staged fluidized bed system for post-combustion CO2 capture using solid sorbents in a continuous temperature swing adsorption process.* Chemical Engineering Science, 2016. **141**: p. 166-174.
22. Roy, S., C.R. Mohanty, and B.C. Meikap, *Multistage Fluidized Bed Reactor Performance Characterization for Adsorption of Carbon Dioxide.* Industrial & Engineering Chemistry Research, 2009. **48**(23): p. 10718-10727.
23. Zanco, S.E., et al., *Modeling of Circulating Fluidized Beds Systems for Post-Combustion CO2 Capture via Temperature Swing Adsorption.* Aiche Journal, 2018. **64**(5): p. 1744-1759.
24. Kim, K., et al., *Moving bed adsorption process with internal heat integration for carbon dioxide capture.* International Journal of Greenhouse Gas Control, 2013. **17**: p. 13-24.
25. Zaabout, A., et al., *Thermodynamic assessment of the swing adsorption reactor cluster (SARC) concept for post-combustion CO2 capture.* International Journal of Greenhouse Gas Control, 2017. **60**: p. 74-92.
26. Riboldi, L. and O. Bolland, *Evaluating Pressure Swing Adsorption as a CO2 separation technique in coal-fired power plants.* International Journal of Greenhouse Gas Control, 2015. **39**: p. 1-16.
27. Wang, L., et al., *Experimental and modeling investigation on post-combustion carbon dioxide capture using zeolite 13X-APG by hybrid VTSA process.* Chemical Engineering Journal, 2012. **197**: p. 151-161.
28. Cloete, S., et al., *The effect of sorbent regeneration enthalpy on the performance of the novel Swing Adsorption Reactor Cluster (SARC) for post-combustion CO2 capture.* Chemical Engineering Journal, 2018.
29. Veneman, R., et al., *Adsorption of H2O and CO2 on supported amine sorbents.* International Journal of Greenhouse Gas Control, 2015. **41**: p. 268-275.

30. Park, Y.-K., et al., *An Energy Exchangeable Solid-sorbent Based Multi-stage Fluidized Bed Process for CO2 Capture.* Energy Procedia, 2017. **114**: p. 2410-2420.